Natural Convection Evaporation from Spherical Particles in High-Temperature Surroundings

D. C. T. PEI and W. H. GAUVIN

Pulp and Paper Research Institute of Canada, Montreal, Quebec, Canada

The prediction of the rate of evaporation of liquids in high-temperature surroundings is important in an increasing number of processes such as spray drying and flash drying, combustion of atomized liquid fuels, cyclone evaporation, and in operations carried out in gas-conveyed systems, such as in the atomized suspension technique (*1*). Theoretically at least, the problem is capable of solution if sufficient knowledge exists concerning the boundary-layer flow pattern and the rate of heat transfer by radiation and convection at every point of the system.

As pointed out by Hoffman (*2*), most of the numerous investigations which have been reported in this field were concerned with low transfer rates and generally fall into two broad classes: measurement of the rate of heat and mass transfer from stationary liquid drops in surroundings at a temperature only moderately higher than that of the drop, and measurement of the rate of heat and mass transfer from liquid and solid spheres in a flowing medium under forced convection conditions.

Virtually all of these studies, the most pertinent of which have been reviewed in reference 2 and will not be listed here, have assumed that the two transfer mechanisms did not affect one another. With work at high rates of mass transfer, Hoffman has, however, shown that the rate of heat transfer is governed by the effect of the evolved vapors on the boundary-layer flow.

The present investigation was undertaken specifically to study the vaporization of liquids at high rates of mass transfer and to provide a better understanding of the complex interaction of the two transfer mechanisms. A theoretical analysis of this problem will first be presented, from which the various dimensionless groups governing the process will be deduced. This will be followed by the description of an experimental study on the rates of evaporation from stationary spheres in high-temperature surroundings.

D. C. T. Pei is with the University of Waterloo, Waterloo, Ontario, Canada. W. H. Gauvin is also with McGill University, Montreal, Quebec, Canada.

ANALYSIS OF PROBLEM

In an analysis of the convective-transfer problem, the fundamental approach is to consider the equations which govern the transfer of momentum, heat, and mass in the boundary layer. To simplify matters the case of two-dimensional incompressible flow along a curved surface will be considered. With a curvilinear orthogonal system of coordinates whose x-axis will be in the direction of the wall, it can be shown that, in general, the boundary-layer equations for a flat wall may be applied to the case of a curved wall as well, provided that there are no large variations in curvature. When applied to a sphere, this approach is only an approximation which should indicate the nature of the dimensionless parameters on which the solution should depend. Thus, assuming constant physical properties, the expressions are Navier-Stokes momentum equation derived from a force balance

$$\rho(u\,\partial u/\partial x + v\,\partial u/\partial y) = \pm g_x \rho \beta(\Delta T) + \mu\,\partial^2 u/\partial y^2 - \partial p/\partial x \quad (1)$$

continuity equation from the material balance

$$\partial u/\partial x + \partial v/\partial y = 0 \quad (2)$$

energy equation from a heat balance, neglecting heat generated by viscous dissipation, and heat generation or absorption in the gas

$$C_p \rho(u\partial T/\partial x + v\partial T/\partial y) = k\,(\partial^2 T/\partial y^2) \quad (3)$$

diffusion equation from a material balance on the diffusing component, neglecting thermal diffusion effects

$$(u\partial c/\partial x + v\partial c/\partial y) = D_v\,(\partial^2 c/\partial y^2) \quad (4)$$

Problems involving simultaneous heat and mass transfer are defined, only at low mass transfer rates, by Equations (1), (2), (3), and (4), with the following boundary conditions:

$$u = 0,\ v = 0,\ T = T_w,\ c = c_w, \quad \text{at } y = 0 \quad (5)$$

$$u = 0,\ du/dy = 0,\ T = T_\alpha,\ dT/dy = 0,\ \text{at } y = \infty \quad c = c_\infty,\ dc/dy = 0 \quad (6)$$

At high mass transfer rates, diffusion need no longer be considered and a heat balance at the surface, where the evaporation process takes place, determines the rate of mass transfer. Thus

$$m\lambda = kA(dT/dy)_{y=0} + q_r \quad (7)$$

where q_r is the net radiative heat transfer to the surface.

Equations (1), (2), and (3) point to the essential feature of natural convection systems, namely that the distribution of temperature and velocity are interdependent. In such systems, the velocity of the fluid is due entirely to the action of buoyancy forces arising from variations in density. Although the nonlinearity of the equations has made direct solution of the temperature and velocity fields impossible, they may be used to derive the dynamic similarity relationships existing between two different systems and thereby allow a prediction of the dimensionless groups associated with those problems.

To achieve dynamic similarity, Equations (1), (2), (3), and (7) must be so transformed that they become identical for the two fields with geometrically similar boundaries. This is possible if dimensionless quantities are introduced. All length terms will be made dimensionless with reference to the diameter of the sphere, and the temperature in the energy equation will be referred to the temperature difference $(T_w - T_\infty)$ between the wall and the fluid at a great distance from the body. But difficulty arises in selecting a suitable characteristic basis for the transformation of velocities. In forced flow, the free-stream velocity is usually selected for this purpose. This basis cannot be used in the case of natural convection where the velocity of the fluid is due entirely to the action of the buoyancy forces and approaches zero beyond the boundary-layer thickness. However, at high mass transfer rate it has been shown that the resulting radial velocity from the sphere is the dominant factor in the rate of heat transfer (*2*). Moreover, this radial velocity is comparable in magnitude with

the fluid velocity induced by natural convection. Hence, in the opinion of the authors, it is justified to use the radial velocity at the surface of the sphere as a suitable basis for the formulation of the dimensionless quantities.

The dimensionless forms of Equations (1), (2), (3), and (7) will then be

$$u_1 \partial u_1/\partial x_1 + v_1 \partial u_1/\partial y_1 = -(1/2)\,\partial p_1/\partial x_1 + \partial^2 u_1/\partial y_1^2 \pm (N_{Gr}/N_{Re}^2)\Theta \quad (8)$$

$$\partial u_1/\partial x_1 + \partial v_1/\partial y_1 = 0 \quad (9)$$

$$u_1 \partial\Theta/\partial x_1 + v_1 \partial\Theta/\partial y_1 = (1/N_{Pr})\,(\partial^2\Theta/\partial y^2) \quad (10)$$

$$N_{Re} = (B'/N_{Pr})\,N_{Nu} \quad (11)$$

The boundary conditions are

$$\text{at } y_1 = 0:\ u_1 = 0,\ v_1 = (N_{Re})^{1/2},\ \Theta = 1 \quad (12)$$

$$\text{at } y_1 = \infty:\ u_1 = 0,\ v_1 = 0,\ \Theta = 0 \quad (13)$$

No attempt was made at this time to solve these equations, although a solution is possible, at least for the case of flat plates. It is to be noted that in this system of equations, the only parameters are the three dimensionless groups, N_{Pr}, (B'/N_{Pr}) and (N_{Gr}/N_{Re}^2). This should prove useful in correlating and interpreting experimental data. It is also clear that, aside from the Prandtl number N_{Pr}, the parameters (B'/N_{Pr}) and (N_{Gr}/N_{Re}^2) are of fundamental importance in the study of simultaneous heat and mass transfer where one transfer mechanism can not be neglected in comparison with the other.

Spalding (3) studied the rate of simultaneous heat and mass transfer from a vertical plate under natural convection conditions, and he attempted to account for the momentum of the vapor leaving the wall by considering the boundary conditions

$$\rho v_w = D_v\,(\partial c/\partial y)_{y=0} \quad (14)$$

In his analysis, Spalding used the Karman-Pohlhausen integral method where velocity, temperature, and concentration profiles in the boundary layer have been approximated by polynomial expansions in terms of the boundary-layer thickness. He also assumed that the thermal diffusivity and molecular diffusivity were equal, and Equations (3) and (4) became identical.

He pointed out that most analyses of convective heat transfer assume that $[1 - (T_\infty/T)] = [(T/T_\infty) - 1]$ and are therefore applicable only to those cases where $(T_\infty - T)$ is small. This assumption may lead to an overestimation of the buoyancy force when temperature differences are large. In his own analysis, he considered $\Delta T/T_\infty = 1$, which means that the buoyancy force is its maximum value at all points of the boundary layer.

Spalding's results are presented in the form of plots of $(\dot{m} C_p/\pi D k)/[D^3 g/\nu^2)\,(N_{Pr}^2)]^{1/4}$ against his transport number B, defined as $(C_p \Delta T/Q)$. A comparison with the stagnant-film hypothesis was also made. He pointed out that this theory (4) will lead to an overestimate of the mass transfer rate of up to 30%.

Godsave (5), in his treatment of the rate of combustion of fuel drops, neglected the convection effects and assumed only radial flow. This implies a spherical symmetrical model which allows radial flow of vapor and radial temperature gradients only. The energy equation can thus be written in the integral form

$$k 4\pi r^2\,(dT/dr)_{r=r_d} + q_r + (q_r)_G = \dot{m}\lambda + \dot{m}\int_{T_w}^{T} C_p\,dT \quad (15)$$

The simplest solution is obtained when $(q_r)_G$, the absorption of radiation in the boundary layer, is neglected and the heat capacity and the thermal conductivity of the gas is assigned an average value. The validity of the former asumption was established by Hoffman (6). Under these conditions, Equation (15) can be integrated to yield

$$1/r_d - 1/r_b = (4\pi k/C_p \dot{m})\,[\ln(1 + C_p \Delta T/\lambda')] \quad (16)$$

Rearranging Equation (16), the evaporation rate can be predicted from the expression

$$\dot{m} = [\ln(1 + B')]/[(C_p/4\pi k)\,(1/r_d - 1/r_b)] \quad (17)$$

where r_b is the effective thickness of the so-called *stagnant film* surrounding the drop. From this equation, Spalding (7) pointed out that the effect of the evaporation rate on heat transfer to the drop is shown to depend on the new parameter which he defined as the transport number, B, as previously mentioned. In his analysis, subject to the above limitations, it is shown that the true Nusselt number $(N_{Nu})_T$ for pure heat transfer, that is, in the absence of evaporation, should be modified to yield the actual Nusselt number $(N_{Nu})_A$ for the case of simultaneous heat and mass transfer, as follows:

$$(N_{Nu})_A/(N_{Nu})_T = [\ln(1 + B)]/B \quad (18)$$

This same analysis has been presented in a slightly different form or extended to include the diffusion of various components by Goldsmith and Penner (8), Marshall (9), Ranz (10), Sleicher and Churchill (11), Spalding (7), and others (12, 13, 14).

Although the above theory based on a spherical symmetrical model has serious drawbacks, it nevertheless provides a better understanding of the process that is actually taking place. Three conclusions may be derived from it. First, at high evaporation rates, the heat capacity of the relatively cold vapor leaving the surface can seriously affect the heat transfer rate. This is shown to depend on the magnitude of the transport number B, modified to include radiation effects. Second, it is clear that the radiant heat transfer can no longer be separated from the conductive and convective heat transfer and treated independently. Third, other things being equal, if for any reason (dT/dr) is increased, $\dot{m}$ will first tend to increase. This will in turn lead to a decrease in $(dT/dr)_{rd}$, and eventually an equilibrium state will be reached. This dynamic balance may be illustrated even better by considering the convection effect characterized by the Grashof number N_{Gr}, as the driving force operating to decrease the boundary-layer thickness and thus increase the temperature gradient $(dT/dr)_{rd}$. This will first lead to an increase of $\dot{m}$ or N_{Re} if expressed in a dimensionless momentum form. As the evaporation rate increases, its immediate effect will be to decrease the temperature gradient. Therefore, as a net result, a new equilibrium is reached which clearly indicates that not Grashof number alone, but the ratio, (N_{Gr}/N_{Re}^2)* is the factor in determining the convection effect on heat transfer when high mass transfer rates persist. Moreover, it is clear that the effect of the convection current on the rate of heat transfer should be considerably less pronounced due to the presence of the evolving vapor. Therefore, for cases where the natural convection effect is small ($N_{Gr} < 10$), such as in the evaporation of small liquid drops, the natural convection can be neglected without appreciable error.

As a result of a growing interest in phenomena associated with transpiration cooling, it is probable that new theoretical contributions may be made in this field. One such different approach was recently taken by Eichhorn (15) who analyzed the effect of mass transfer on free convection. A vertical flat plate from which was ejected a fluid with the same physical properties

* In the Grashof number the group $Dg\beta(\Delta T/2)$ represents the average buoyancy potential energy. For frictionless flow this can be replaced by a kinetic energy of $v^2/2$, if the pressure gradient is neglected, and thus

$$N_{Gr} = D^2 v^2/\nu^2 = N_{Re}^2$$

as the quiescent surroundings, but at a different temperature, was considered. Following the procedure developed by Eckert (*16*) and Brown (*17, 18*), Equations (1), (2), and (3) were first reduced to

$$f''' + 3ff'' - 2f'^2 + \Theta = 0 \quad (19)$$

$$\Theta'' + 3\,N_{Pr}\,f\,\Theta' = 0 \quad (20)$$

where f and Θ are the dimensionless stream function and temperature, respectively, both functions of η defined by

$$\eta = (u/x)\,(N_{Gr}/4)^{1/4} \quad (21)$$

The velocities in x and y directions and the temperature distribution are given by

$$u = (4\nu/x)\,(N_{Gr}/4)^{1/2}\,f' \quad (22)$$

$$v = -\,(\nu/x)\,(N_{Gr}/4)^{1/4}\,(3f - \eta f') \quad (23)$$

$$\Theta = (T - T_\infty)/(T_w - T_\infty) \quad (24)$$

respectively. The boundary conditions are

$$f = f_w,\ f' = 0,\ \Theta = 1, \text{ at } \eta = 0$$
$$f' = \infty,\ \Theta = 0, \text{ at } \eta = \infty \quad (25)$$

Solutions to Equations (19) and (20) for $N_{Pr} = 0.73$ were obtained numerically on a computer for several values of f_w ranging from strong suction to strong blowing. The interesting conclusions drawn from these solutions are that the skin friction is only slightly affected by the mass transfer; the effect of mass transfer on the heat transfer is most pronounced, and the heat transfer rate is essentially zero at a high rate of blowing through the porous wall.

However, it must be pointed out that the above analysis has its theoretical limitations. According to Schlichting, the mathematical study of the laminar boundary layer with suction or blowing generally assumes that the fluid removed or injected is so small that only the immediate neighborhood of the wall is affected. This is equivalent to saying that, in general for forced convection, the ratio of the suction or blowing velocity to the free-stream velocity (v_w/U_∞) is very small, say in the order of 0.0001 to 0.01; whereas in the case of natural convection, the convective currents, induced by the difference in density, are restricted to the boundary layer. Therefore any fluid removed or injected through the wall in this case has a much more pronounced effect on the boundary layer than in the case where forced convection is dominating. Great caution should therefore be taken in interpreting Eichhorn's theoretical predictions.

Attention has so far been directed to the theoretical aspects of the problem. Consideration will now be given to some of the more pertinent experimental investigations in this field. Most of these studies have been concerned with measurements of the rates of vaporization from small stationary liquid drops suspended in a quiescent atmosphere (*1, 19, 20*). The evaporation rate was found to depend directly on the drop diameter and, based on this simple relationship, experimental results have invariably been reported in terms of the evaporation constant which is defined as the slope of the plot of D^2. Similar experimental techniques have been used for determining combustion rates of fuel drops (*21, 22, 23, 24, 25, 26*). However, since the variables required for an analysis of this process are quite often not accurately known, the fundamental mechanism of drop evaporation in this case is difficult to isolate and to evaluate quantitatively, and the extensive literature available on this subject has therefore been excluded.

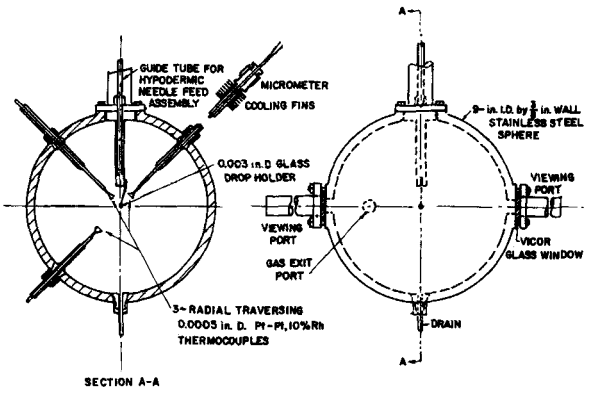

Fig. 1. Diagrammatic sketch of the 9-in. I.D. sphere assembly.

Nishiwaki (*19*) studied the rates of evaporation from drops of water, methanol, and heptane. The experimental values were found to agree with those predicted by Equation (17), modified to include thermal radiation effects. The values of (r_b/r_d) measured from Schlieren photographs were found to be approximately equal to 3 for various temperatures and times, regardless of the kind of liquid used.

In their theoretical analysis of the evaporation process, Tanasawa and Kobayasi (*27*) considered the evaporation period as being the sum of preheating and an evaporative time interval. Each period was assumed to be independent of the other. During the preheating period the temperature of the drop was allowed to reach an arbitrary temperature T_s and the Nusselt number was assumed to be approximately 2.0. During the evaporative period, a finite arbitrary portion of the mass of the drop was assumed to vaporize causing the drop temperature to fall. This cycle was repeated until evaporation was complete. Kobayasi (*20*), at a later date, reported the rates of evaporation of twelve pure organic liquids and five blends of petroleum products from stationary drops in air at temperatures from 50° to 800°C. In the case of water, methanol, and benzene only, the results were compared with the theory and found to be in fair agreement. It is of interest to note that the evaporation constants reported by Kobayasi for water and for methanol in particular were higher than those obtained by Nishiwaki.

Hoffman (*2*) in his studies of the evaporation rate of stationary drops of water, methanol, cumene, pentane, and benzene found that his data agreed well with those reported by Kobayasi. However, in his analysis he found no dependency of Nusselt number on the Grashof number*. He concluded that although buoyancy effects undoubtedly exist in the boundary layer, they could not be accounted for in the conventional way, that is, by means of the Grashof number. Therefore, rather than correlating the data by using the Nusselt number, he proposed the following expression:

$$(\dot{m}\,C_p/\pi D k_f)\,(N_{Pr})^{-1/3} = 3.2B^{0.97} \quad (26)$$

He pointed out that the group $(\dot{m}\,C_p/\pi D k_f)$ was equivalent to the product $(N_{Re} \cdot N_{Pr})$, or the Peclet number for the evolved vapor, based on the radial velocity. The accuracy of this expression in predicting the evaporation rates clearly inferred that the mass rate of vapor evolution depended on the evaporation rate itself.

Based on the theoretical considerations which have been presented and on the experimental evidence available, it can be concluded that any attempt to formulate a sound correlation for the mechanism of natural convection at high mass transfer rates should take into account four major factors.

* The Nusselt number for heat transfer by natural convection is known to depend on $(Ga_r)^n$, for which Ranz and Marshall (*28*) suggest $n = 0.25$. Therefore, the evaporation rate should be a function of D^{3n+1}. Hoffman, however, found it to be a function of D.

1. The mass flow rate of evolved vapors undoubtedly affects the flow pattern in the boundary layer. In quiescent atmospheres, the radial vapor velocity at the drop surface may be comparable in magnitude to the free convection velocity. As a result, the effect of the convective current on the rate of the heat transfer cannot be represented by the Grashof number alone but by the ratio (N_{Gr}/N_{Re}^2).

2. As the relatively cold vapor moves away from the surface into the high temperature surroundings, its sensible heat content must increase and cannot be neglected in comparison with the latent heat of vaporization. Therefore, the Nusselt number for heat transfer must be corrected as indicated by Equation (18).

3. At high temperatures, the radiant transfer may contribute as much as 80% of the total thermal energy required for the evaporation process. Although Godsave (5) neglected radiation in his analysis, he proposed that it be considered as reducing the heat requirement necessary for the evaporation of the drop. Thus, the latent heat of vaporization can be expressed as

$$\lambda' = \lambda - (q_r/m) \qquad (27)$$

4. Because of the large temperature differences involved, there is some doubt as to what mean temperature should be used to evaluate the physical properties of the vapor. Douglas and Churchill (29) showed that most of the published high-temperature data could be reconciled if the fluid properties were evaluated at the average boundary layer temperature. This was also suggested by Jakob (30).

It must be emphasized that none of the studies so far reported in the literature have taken into account all four factors in the interpretation of their data. The task of the present investigation was therefore twofold: to verify the validity of the dimensionless groups predicted from the theoretical analysis for the correlation of the experimental heat transfer data, and to incorporate in this correlation the four factors which have just been discussed, namely: use of the group (N_{Gr}/N_{Re}^2) as the main variable and of the corrected Nusselt number $(N_{Nu})_T$ for the heat transfer-rate-determining term, inclusion of radiant heat transmission in the transfer equations, and finally estimation of the boundary layer properties at the proper mean temperature.

EXPERIMENTAL

The experimental investigation involved measurement of the rate of evaporation of three different liquids, water, benzene, and methanol, from stationary porous hollow spheres, ¼ to ½ in. in diam., in a quiescent atmosphere consisting of their own vapor, at temperatures ranging from 400° to 1,000°K.

Equipment

The main components of the experimental equipment used in the present study were those described by Hoffman in his thesis (31). Only a brief description will be given here. The 9-in. *I.D.* stainless steel sphere shown in Figure 1 was made up of two hemispheres each equipped with opposite viewing ports and was designed to operate at temperatures up to 1,500°F. and pressures up to 10 atm. The sphere assembly was housed in a stainless steel box equipped with Nichrome wire heaters. The temperature of the system was controlled by a pyrovane proportional controller, and the whole assembly was insulated with 6 in. of Fiberfrax.

To measure the steady state evaporation rate of a liquid from a porous sphere, a thin film of the liquid must be maintained at the surface by continuous feeding. To be effective, the method of feeding must be so designed as to prevent the liquid from boiling before it reaches the sphere, and interference with the flow of the natural convection currents around the sphere must be avoided. A feeding unit which appeared to meet these requirements was designed and constructed.

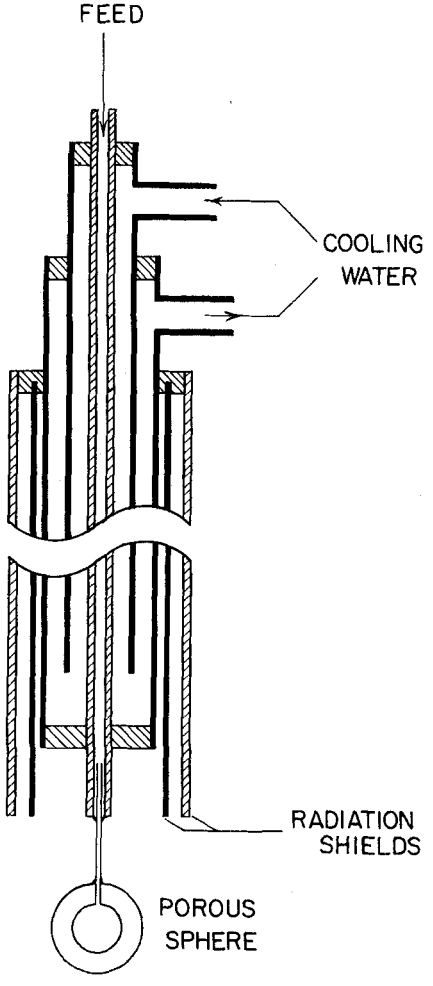

Fig. 2. Diagrammatic sketch of the liquid feeding assembly.

As shown in Figure 2, it consisted of a 1/16-in. stainless steel tube, enclosed in a cooling water jacket through which the test liquid was injected. Two concentric radiation shields about 0.01 in. apart provided the necessary insulation from the high-temperature surroundings. The whole assembly was tested in an open furnace, and although the outer shield was glowing red, the cooling water temperature in the jacket rose by less than 10°C.

For ease of handling, fine hypodermic needles sealed with epoxy into the porous spheres were joined to the feeding assembly by soldering. To minimize the interference of the holder on the flow pattern around the evaporating sphere, a minimum distance of ½-in. was maintained between the sphere and the holder.

The porous hollow spheres (¼, ⅜, and ½ in. in diam.) were made of diatomaceous earth (Celite) without the binding clay, to increase its porosity. Thus prepared, this material absorbs about three times its own weight of liquid before reaching saturation. It is interesting to note that despite its exceptionally high absorptive capacity for liquids, Celite is nearly nonhygroscopic.

Three 0.0005-in. platinum platinum-10% rhodium thermocouples were provided for mapping the temperature profiles around the sphere. The thermocouples could be moved by a micrometer screw outside the sphere, so that the thermocouple junction in the plane of the great circle of the sphere could traverse the region immediately surrounding the sphere in a direction of constant polar angle. The position of the thermocouple relative to the surface of the sphere was determined within 0.005 in. by means of a microvernier. The 0.0005-in. wires were fused together using a microtorch. The thermocouples were calibrated against an accurate standard thermometer over the range of temperatures between 100° and 400°C.

The temperature-recording system consisted of a precision potentiometer combined with a high-speed strip-chart recorder with a pen speed of one quarter second for full-scale travel. Switches were used to give any desired combination of temperature readings and also to permit convenient standardization of the recorder against the potentiometer.

It soon became evident that a qualitative visualization of the flow pattern of the evolved vapor would be of great assistance in the interpretation of the mass transfer data. A complete optical bench was therefore developed to take Schlieren photographs of the evaporating sphere which has been described elsewhere (42).

Procedure

The stainless steel was heated up and maintained at the desired temperature for about 2 hr. prior to the experimental test. During this time, the sphere was purged of its contained gas atmosphere twice by injecting approximately 75 ml. of the liquid under study. When all three thermocouples registered the same temperature throughout a complete traverse of the atmosphere, the feeding assembly with

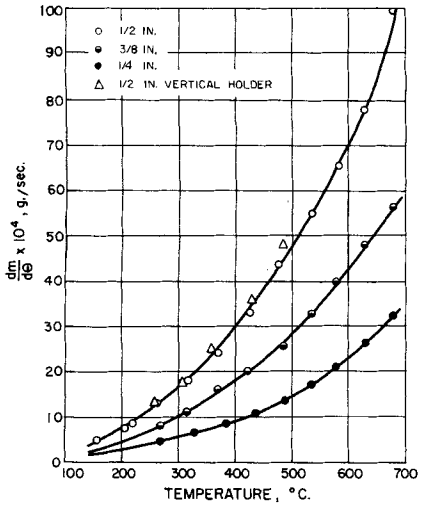

Fig. 3. Evaporation rate data for water.

the attached porous sphere was introduced. The liquid from a calibrated glass cylinder was fed to the sphere through a needle valve. Since the whole system was under pressure (approximately 15 lb./sq. in. gauge), it may be safely assumed that the change of the liquid level in the calibrated glass container had very little effect on the actual rate of flow. The feed was adjusted, by observation through the viewing ports and manipulation of the needle valve, to give just enough liquid to maintain a thin liquid film on the surface of the sphere. The feed rate was then recorded every 5 min. during a period of 1 hr. Certain runs were repeated under identical conditions, and the maximum variation in evaporation rate was found to be 3%.

After steady state had been reached the temperature profiles around the sphere were mapped and recorded on the strip-chart recorder. For runs numbers 1 to 9, in which the feeding assembly was introduced from the top, two temperature profiles were made: one at 45 deg. and the other at 135 deg. from the lower stagnation point. To minimize interference with the natural convection currents, the feeding assembly in the remaining runs was introduced at an angle of 45 deg. from the lower stagnation point. This was achieved by inserting the feed tube through one of the thermocouple ports in the lower half of the stainless steel sphere. In these runs, the temperature profiles were taken at 135 deg. from the lower stagnation point.

Substances Investigated

The effect of mass transfer on heat transfer may be expected to be particularly pronounced when the dimensionless group B' is large. In other words, significant perturbations should arise either when the ambient temperature T_∞ is high or when the latent heat of the liquid is small. Based on these considerations, and also on the availability of the liquids in pure form and a knowledge of their physical properties, distilled water, methanol, and benzene (both analytical reagent grade) were chosen as the most suitable substances to be studied.

The physical properties of steam have been measured and reported by Keyes (32). However, the data for the organic vapor at high temperatures presented a more difficult problem. They were obtained mainly from a critical review of the literature data and the extrapolation of the data collected by Reid and Sherwood (33), Vines (34), Vines and Bennett (35), Montgomery and De Vries (36) and De Vries and Collins (37).

RESULTS

The experimental rates of evaporation are summarized in Table 1* and plotted in Figures 3, 4, and 5. All experiments were carried out at atmospheric pressure, and the temperature ranged from 400° to 1,000°K.

Values of thermocouple temperatures around the spheres are plotted in Figures 6 and 7 as a function of a dimensionless ratio (r/r_d), where r is the radial distance from the center of the sphere. Short, Brown, and Sage (38), in their study of local thermal transfer from spheres, have given a detailed discussion of the errors involved in the measurement of boundary-layer temperature profiles by means of thermocouples. The most serious one results from significant thermal transfer by conduction from the thermocouple junction to the sphere when the distance between the two is of the order of the boundary-layer thickness on the former. Also, as a result of large temperature gradients along the wire, some thermal transfer by conduction must necessarily occur. The interference on the boundary-layer flow caused by the wake of the thermocouple junction and the radiation from the surroundings to the wires may similarly be significant in the present work, since the 0.0005-in. thermocouple wires were joined by direct fusion and the resulting junction was of the order of 0.0015 in. in diameter. In view of these uncertainties and the lack of available information required for corrections, only a selected number of profiles were taken, and they are reported here as a qualitative study only.

* Tabular material has been deposited as document 7523 with the American Documentation Institute, Photoduplication Service, Library of Congress, Washington 25, D. C., and may be obtained for $1.25 for photoprints or for 35-mm microfilm.

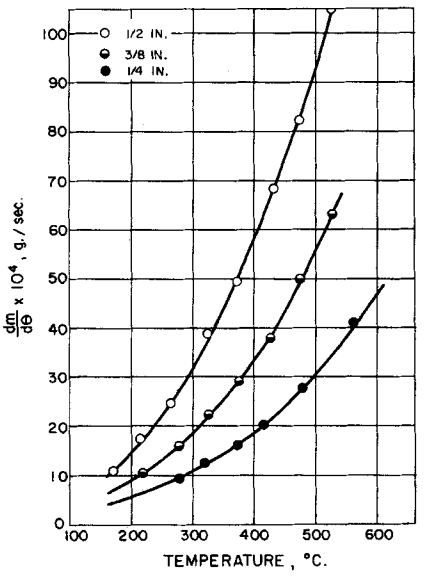

Fig. 4. Evaporation rate data for methanol.

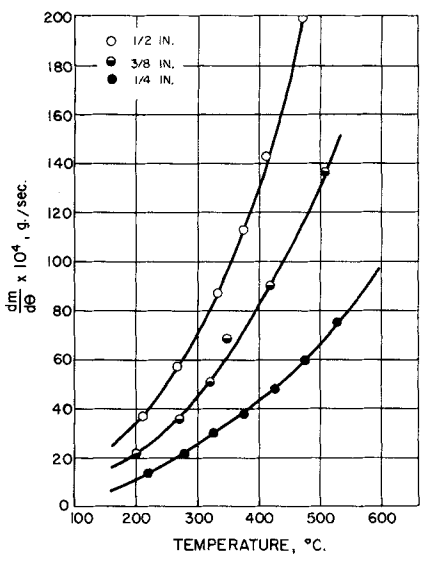

Fig. 5. Evaporation rate data for benzene.

TREATMENT AND DISCUSSION OF DATA

The total interfacial heat flux from the gas to the liquid film on the surface of a porous sphere can be obtained from the following energy balance:

$$m\lambda - [q_r + (q_r)_G] = kA(dT/dr)_{r=r_d} = h_A A \Delta T \quad (28)$$

Hoffman (6) estimated the magnitude of the radiation absorbed by the relatively colder boundary layer and found $(q_r)_G$ to be negligibly small. Therefore, the thermal radiation received by the sphere will be essentially the same as that which it would receive if it were in a nonabsorbing medium. The radiation absorbed by the sphere is then given by:

$$q_r = \alpha_p \sigma A (T_\infty^4 - T_w^4) \quad (29)$$

The absorptivity of the various liquids on porous surfaces was not available from the literature at the time of this study. However, it has been known for some time that the absorptivity of liquid films is a function of their thickness. This leads to the belief that the porous surface background may be an important factor in the absorption of thermal radiation. The main chemical composition of Celite is 89% silica, 4% alumina and 1.5% iron oxide. The particle size is in the range of 4 to

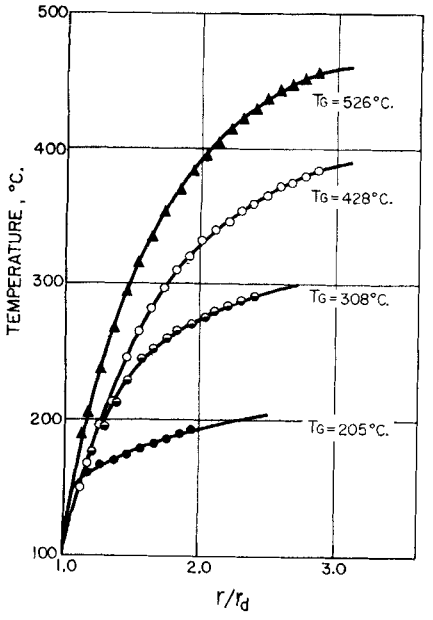

Fig. 6. Temperature profiles of water vapor around a ½-in. sphere (45 deg. from the lower stagnation point).

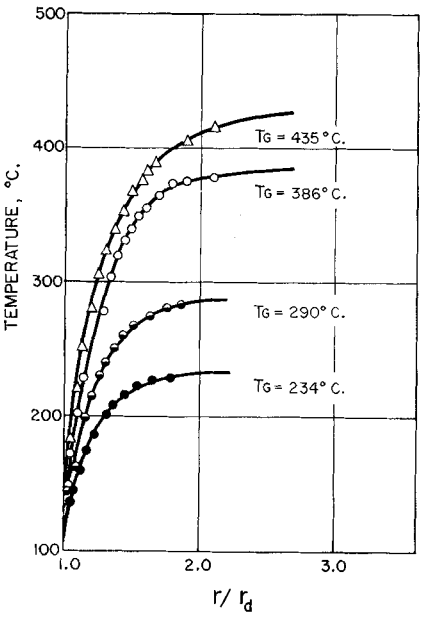

Fig. 7. Temperature profiles of water vapor around a ½-in. sphere (135 deg. from the lower stagnation point).

10 μ. Michaud (39) studied the effect of mean grain size and iron oxide impurities on the absorptivity of silica-alumina refractories, and his results showed that the absorptivity of a refractory composed of 60% silica, 26% alumina, and 1.6% iron oxide had a value of 0.73. Water is decidedly opaque to thermal radiation and an absorptivity as high as 0.9 has been commonly used. The same may hold for methanol and benzene. Owing to the uncertainty concerning the exact thickness of the liquid film, it was felt that the use of an average value of 0.8 best represented the combined effects of the liquid and surface absorptivities. Moreover, this value of α_p correlated the data with minimum deviation from the relationship which will be proposed later.

Rearranging in the form of dimensionless groups, Equation (28) becomes

$$(N_{Nu})_A = h_A D/k = (\dot{m}\, C_p/\pi Dk)/B' \qquad (30)$$

where

$$B' = (C_p \Delta T)/(\lambda - q_r/\dot{m})$$

Combining Equations (29) and (18) to obtain the true Nusselt number $(N_{Nu})_T$ for pure heat transfer

$$(N_{Nu})_T = \dot{m}\, C_p/\pi Dk \ln (1 + B') \qquad (31)$$

The gas properties were evaluated at the average film temperature.

The true Nusselt number, $(N_{Nu})_T$, was first plotted against the buoyancy force represented by the Grashof number, as shown in Figure 8. The correlation proposed by Ranz and Marshall (28) for natural convection heat transfer at small rates of mass transfer was also included for comparison. A definite pattern in the variations of the true Nusselt number can be clearly observed for each set of data, indicating the effect of mass transfer rate.

An attempt was also made to correlate the experimental results by means of Hoffman's method (2). A straight line could be drawn through the data and the expression for the regression line was

$$(\dot{m}\, C_p/\pi Dk)\,(N_{Pr})^{-1/3} = 5.4\,(B')^{0.65} \qquad (32)$$

with a root mean square deviation of 22.8%. This differs from the correlation proposed by Hoffman, extrapolated to the range of the present study, on two counts: it leads to somewhat higher rates of mass transfer than those predicted by Hoffman, and the dependence on B' is not as pronounced. Reasons for these discrepancies may be summarized as follows:

1. Hoffman's range of Grashof numbers was less than 10. The Grashof number in the present study was considerably higher, of the order of 10^2 to 10^4. Since it has been shown in the analysis that this dimensionless group is one of the governing factors for the transfer rate, Hoffman's correlation cannot be expected to cover a large range of Grashof numbers, although it may be quite adequate at low values of the latter.

2. Hoffman used B in his correlation which does not differ too much from B' for small droplets. Thus for the liquid drops which he used, 0.5 to 1.2 mm. in diam., approximately, the contribution from radiation was in the range from 10 to 35%. However, in the case of the larger spheres used in the present investigation this contribution was as high as 80%* of the total heat transfer rate, in which case B' will differ from B significantly. It has been shown in the analysis that B' should be the proper parameter to use.

3. It is interesting to note that, if the power of B appearing in Hoffman's correlation, Equation (26), is taken to be unity, and combined with Equation (30), the result is:

$$(N_{Nu})_A = 3.2\, Pr^{1/3} \qquad (33)$$

Since the Prandtl number for most liquid vapors is in the neighborhood of unity, the above equation would indicate that in Hoffman's case the apparent Nusselt number was close to a value of 3.2. In the present study the apparent Nusselt number varied from 3 to 7, as could be expected since a much wider range of Grashof numbers (over thirtyfold) was covered.

It might be instructive to attempt to establish the dependency of heat transfer on natural convection by comparing the actual measured temperature profiles with those calculated from Equation (16) in which the convection effect is neglected. As shown in Figure 9, for $r_b/r_d < 1.2$ the calculated curve, dotted line, lies between

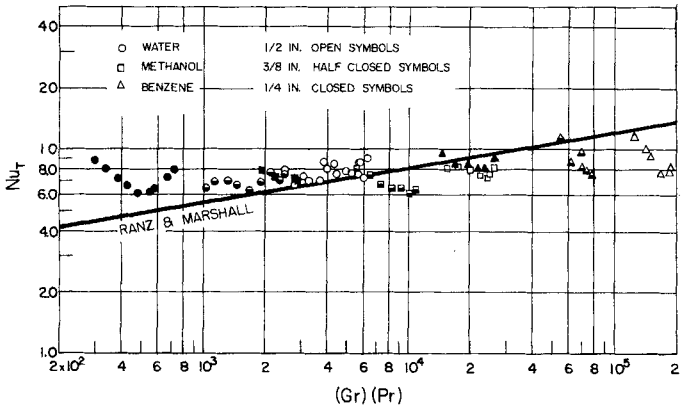

Fig. 8. Plot of true Nusselt numbers against Grashof number ($Pr = 1$).

* It is obvious that although convection heat transfer varies as the first power of D, radiation transmission is proportional to D^2.

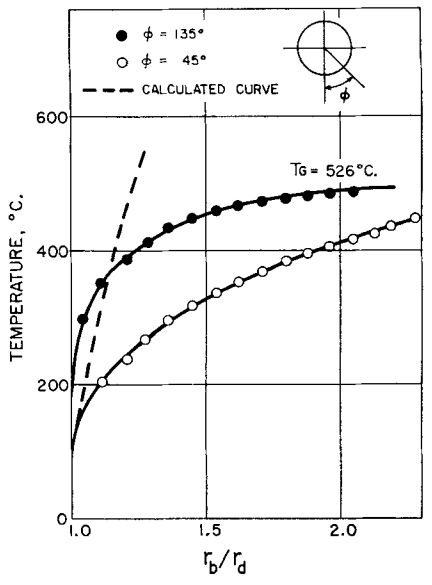

Fig. 9. Comparison of calculated temperature profile of water vapor from Equation (16) (R_d = ½-in.).

the experimental temperature profiles for the upper and lower half of the porous sphere respectively. This clearly indicates the presence of the natural convection effect: at the top of the sphere, the boundary layer is depleted by the convection currents, resulting in a steeper temperature gradient. The opposite behavior applies for the lower part of the sphere. At $r_b/r_d > 1.2$, the cold vapor decreases the temperature gradient. Unfortunately, the uncertainties involved in the thermocouple readings prevented any quantitative analysis of the local thermal transport values.

It should be noted that in most cases the solutions of the temperature and velocity fields in the boundary layer are not required. Examination of the boundary-layer equations from the point of view of the principle of similarity indicates the dimensionless groups on which the solution must depend. Thus, the solutions of Equations (1), (2), and (3), together with Equation (7) which determines the mass transfer rate, depend on the following dimensionless groups: (N_{Gr}/N_{Re}^2), (B'/N_{Pr}) and N_{Pr}. The form of the correlation involving these groups is suggested by the solution for the flat-plate problem for incompressible flow and $N_{Pr} \neq 1$ (*43*), modified to include the groups predicted by the analysis. Accordingly, $[(N_{Nu})_T/(N_{Re})^{1/2}]\ [B'/(N_{Pr})^{1/3}]$ was plotted against (N_{Gr}/N_{Re}^2) as shown in Figure 10. All the data correlate satisfactorily with a root mean square error of 6.5%. The expression for the proposed correlation is

$$[(N_{Nu})_T/(N_{Re})^{1/2}][B'/(N_{Pr})^{1/3}] = 3.32\ (N_{Gr}/N_{Re}^2)^{0.007} \quad (34)$$

The data of Hoffman (*2*), Nishiwaki (*19*) and Kobayasi (*20*) for water, benzene, and methanol were also evaluated on the basis of the above correlation. The regression line in this case is somewhat different and is represented by the following expression with an average deviation of 5.9%:

$$[(N_{Nu})_T/(N_{Re})^{1/2}][B'/(N_{Pr})^{1/3}] = 2.11\ (N_{Gr}/N_{Re}^2)^{0.077} \quad (35)$$

In the establishment of the latter correlation, the following points should be noted:

1. The data of these three workers were obtained under unsteady conditions. The recession of the boundary layer might have had an effect on the results, as discussed by Sparrow and Gregg (*40*).
2. The absorptivity of the liquid droplets was taken as 0.9 by the three workers, whereas the measurement of Brown (*41*) indicates slightly lower value for water films 0.5 mm. thick.
3. The sensible heat of the liquid droplets was neglected in these investigations. Although this factor may be small, particularly in the case of water, it is certainly not negligible.

CONCLUSIONS

It is recognized that at small mass transfer rates the flow of material across the interface is important only in calculating the fluxes of the different species across the boundary. The distortion of the velocity and concentration profiles by mass transfer may be neglected, which makes it possible to solve many mass transfer problems by analogy with corresponding problems in heat transfer. The converse is also true. This important analogy permits one to derive mass transfer correlations from heat transfer correlations for equivalent boundary conditions by merely substituting N_{Sh} for N_{Nu} and N_{Sc} for N_{Pr} for almost any flow geometry and for laminar or sometimes for turbulent flows.

In the case of high mass transfer, there are, in general, two approaches to the problem: to evaluate correction factors by which h and k_g may be multiplied to obtain the corrected coefficients, and to correlate the results on the basis of Godsave's spherical model, conduction across the boundary layer controlling. The main limitation to the former lies in the assumption that the boundary is unaffected by mass transfer, whereas the latter assumes that the convection effect is negligible.

In the present investigation, a third approach has been presented. The theoretical analysis of the boundary-layer equations based on a finite radial velocity of vapor at the surface of the sphere revealed that the effect of convective currents can be accounted for by the parameter (N_{Gr}/N_{Re}^2). Accordingly, the experimental results of the evaporation rates were satisfactorily correlated by the expression

$$[(N_{Nu})_T/(N_{Re})^{1/2}][B'/(N_{Pr})^{1/3}] = 3.32\ (N_{Gr}/N_{Re}^2)^{0.007} \quad (34)$$

Although $(N_{Nu})_T$ varied only from 6.05 to 11.5, B' covered a range from 0.166 to 9.63 and N_{Gr} from 297 to 10,250. The accuracy of this expression is quite encouraging, particularly in view of the uncertainties concerning the physical properties of benzene and methanol. Since it has been established experimentally that the evaporation rates of stationary drops in high-temperature surroundings depended on the mass rate of vapor evolution, the weak dependence of the rates of heat transfer on (N_{Gr}/N_{Re}^2) is not surprising. This explains the fact that a number of published experimental studies could be successfully correlated by excluding the convection effect within a limited range of Grashof numbers.

Moreover, the above correlation gives support to the following points:

1. The vapor evolution thickens the boundary layer around the sphere and therefore controls the heat transfer rate.
2. At high temperatures, the sensible heat of the evolved vapor is no longer small and hence the Nusselt

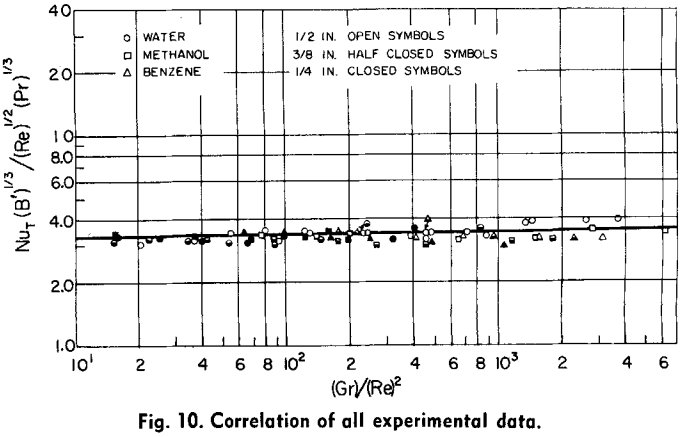

Fig. 10. Correlation of all experimental data.

number must be modified to give its true value.

3. The buoyancy force existing in the boundary layer is considerably less pronounced than in the case where the mass transfer rate is small. It therefore cannot be accounted for by means of the Grashof number alone.

4. The radiant heat transfer contribution can no longer be considered separately from that due to convection and conduction.

5. The variation of the physical properties may be accounted for satisfactorily by using the values calculated at the arithmetic mean film temperatures across the boundary layer.

It might be argued that the proposed correlation cannot be extrapolated to the case of heat transfer where the vapor Reynolds number is negligibly small, since it would assume an indeterminate form. It is not believed, however, that this criticism is well-founded nor does it invalidate the correlation, since the latter was derived on the basis of a finite surface vapor velocity acting to modify the fluid dynamic behavior in the boundary layer. Owing to the very nature of the effect of mass transfer on the rate of heat transfer, it is doubtful whether a single correlation could be found which would cover the effect of mass transfer, and at the same time include pure natural convection heat transfer.

It is even more difficult to predict at what minimum mass transfer rate Equation (34) begins to apply. Part of the difficulty is due to the fact that as ΔT increases, N_{Gr} for a vapor increases quite rapidly at first, then passes through a maximum at a ΔT in the range of 125° to 150°C., for the materials investigated, and then decreases steadily as ΔT continues to increase, since the kinematic viscosity increases rather markedly with temperature. Thus any prediction involving the Grashof number might not be a simple one and cannot be obtained from the present work which was carried out entirely in the range of decreasing N_{Gr}. It is hoped that further studies which are currently under way in this laboratory will help to elucidate this important point.

ACKNOWLEDGMENT

Financial assistance to D. C. T. Pei from the Shell Oil Company of Canada, Ltd., Canadian Refractories, Ltd., and the National Research Council in the form of bursaries and fellowships, is gratefully acknowledged. Recognition is also due to the Pulp and Paper Research Institute of Canada for the extensive use of its facilities.

NOTATION

A = area, sq. ft.
c = concentration of diffusing component, lb./cu. ft.
C_p = heat capacity, (B.t.u.)/(lb.) (°F.)
D = diameter, ft.
D_v = mass diffusivity, sq. ft./sec., or sq. ft./hr.
f = dimensionless stream function
f', f'', f''' = first, second, and third derivatives of f with respect to η
g = gravitational constant, ft./(hr.)^2
h = heat transfer coefficient, (B.t.u.)/(hr.) (sq. ft.) (°F.)
k = thermal conductivity, (B.t.u.)/(hr.) (ft.) (°F.)
K = constant
k_g = mass transfer coefficient, (lb. moles)/(hr.) (sq. ft.) (Δp)
L = characteristic length, ft.
m = evaporation, g. or lb.
$\dot{m}\,(dm/d\theta)$ = evaporation rate, g./sec. or lb./hr.
p = pressure, lb./sq. ft.
q = heat transfer rate, B.t.u./hr.
Q = heat conducted from gas to body, per unit mass of vapor evolved
r = radius, ft.
r_d = radius of a sphere, ft.
r_b = radius of effective spherical boundary layer, ft.
T = absolute temperature, °R
u = component velocity in x-direction, ft./sec.
U = free-stream velocity, ft./sec.
v = component velocity in y-direction, ft./sec.
x, y = distance in Cartesian coordinate system, ft.

Greek Letters

α_p = absorptivity of particle, dimensionless
β = coefficient of volume expansion, 1/°R
η = boundary-layer coordinate, dimensionless
θ = time, hr.
Θ = temperature difference ratio, dimensionless, Equation (24)
Θ', Θ'' = first and second derivatives of Θ with respect to η
λ = latent heat of vaporization, B.t.u./lb.
λ' = modified latent heat of vaporization, B.t.u./lb., Equation (27)
ρ = density, lb./cu. ft.
σ = Stefan-Boltzmann constant: 0.173×10^{-8}, (B.t.u.)/(hr.) (sq. ft.) (°R.)^4
μ = absolute viscosity, (lb.)/(ft.) (sec.), or (lb.)/(ft.) (hr.)
γ = kinematic viscosity, sq. ft./hr.

Dimensionless Groups

B = Spalding's transport number: $C_p\Delta T/\lambda$
B' = Spalding's modified transport number: $C_p\Delta T/\lambda'$
N_{Gr} = Grashof number: $D^3g\beta\Delta T/\nu^2$
N_{Nu} = Nusselt number: hD/k
N_{Pr} = Prandtl number: $C_p\mu/k$
N_{Re} = Reynolds number: Dv_w/ν
p_1 = $p/\rho v_w^2$
u_1 = u/v_w
v_1 = $(v/v_w)\ (N_{Re})^{1/2}$
x_1 = x/D
y_1 = $(y/D)\ (N_{Re})^{1/2}$

Subscripts

A = actual
b = boundary layer
d = drop
G = gas
r = radiation
T = true
w = wall
x = x-direction
y = y-direction
∞ = main stream

LITERATURE CITED

1. Gauvin, W. H., and J. J. O. Gravel, Paper presented at the Third Congress of the European Federation of Chemical Engineering, London, England (June 1962).
2. Hoffman, T. W., and W. H. Gauvin, *Can. J. Chem. Eng.*, 38, 129-137 (1960).
3. Spalding, D. B., *Proc. Roy. Soc. (London)*, **A221**, 78 (1954).
4. Spalding, D. B., *Fourth Symposium on Combustion and Flame Phenomenon*, Massachusetts.
5. Godsave, G. A. E., *Report No. R66*, National Gas Turbine Establishment (N.G.T.E.), England (March, 1950), *Report No. R87*, N.G.T.E., England (April, 1951), *Report No. R88*, N.G.T.E., England (August, 1952), *Report No. R125*, N.G.T.E., England (October, 1952).
6. Hoffman, T. W., and W. H. Gauvin, *Can. J. Chem. Eng.*, 39, No. 6, p. 252 (1961).
7. Spalding, D. B., *Fourth Symposium (International) on Combustion*, p. 847, Williams and Wilkins, Baltimore, Maryland (1953).
8. Goldsmith, M., and S. S. Penner, *Jet Propulsion*, 24, 245 (1954).
9. Marshall, W. R., Jr., *Chem. in Canada*, 7, 37 (1955).
10. Ranz, W. E., *Trans. Am. Soc. Mech. Engrs.*, 78, 909 (1956).
11. Sleicher, C. A., Jr., and S. W. Churchill, *Ind. Eng. Chem.*, 48, 1819 (1956).
12. Kumagai, Seiichiro, and Itsuro Kimura, *Sc. of Mach.*, 3, 431 (1951), 4, 337 (1952).
13. El Wakil, M. M., O. A. Uyehara, and P. S. Myers, Nat'l Advisory Comm. Aeronaut *Tech. Note 3179* (1954).
14. Okazaki, Takuro, and Maruzuke Gomi, *Trans. Soc. Mech. Engrs. (Japan)*, 19, 88 (1953).
15. Eichhorn, R., *J. Heat Transfer, Trans. Am. Soc. Mech. Engrs.*, Series C, 82, 260 (1960).
16. Eckert, E. R. G., *Air Material Command Tech. Rep't., No. 5646* (1947).
17. Brown, W. B., *Am. Soc. Mech. Engrs. Proc., First U.S. Nat. Cong. Appl. Mech.*, 843-852 (1952).

18. Brown, W. B., and J. N. B. Livingood, Nat'l Advisory Comm. Aeronaut. *Tech. Note 2800* (1952).
19. Nishiwaki, Niichi, *Fifth Symposium on Combustion (International)*, p. 148, Reinhold, New York (1955).
20. Kobayasi, Kiyoshi, *Trans. Soc. Mech. Engrs. (Japan)*, **20**, No. 100, 826-831 (1954).
21. Priem, R. J., G. L. Borman, M. M. El. Wakil, O. A. Uyehara, and P. S. Myers, Nat'l Advisory Comm. Aeronaut. *Tech. Note 3988* (1957).
22. Agoston, G. A., H. Wise, and W. A. Rosser, *Sixth Symposium on Combustion*, p. 708, Reinhold, New York (1957).
23. Rex, J. F., A. E. Fuhs, and S. S. Penner, *Jet Propulsion* **26**, 179 (1959).
24. Diederichsen, J. and A. R. Hall, *Fourth Symposium (International) on Combustion*, p. 837, Williams and Wilkins, Baltimore, Maryland (1953).
25. *Sixth Symposium (International) on Combustion*, p. 123-133, Reinhold, New York (1957).
26. *Seventh Symposium (International) on Combustion*, p. 399-406, Academic Press, New York (1959).
27. Tanasawa, Y., and K. Kobayasi, *Tech. Rep. of Tohoku Univ.*, **14**, No. 2, **15**, No. 55 (1950).
28. Ranz, W. E., and W. R. Marshall, Jr., *Chem. Eng. Progr.*, **48**, 141, 173 (1952).
29. Douglas, W. J. M., and S. W. Churchill, *Chem. Eng. Progr. Symposium Ser. No. 18*, **52** (1956).
30. Max Jakob, "Heat Transfer", Vol. 1, p. 497, Wiley, New York (1950).
31. Hoffman, T. W., Ph.D. thesis, McGill Univ., Montreal, Quebec, Canada (1959).
32. Keyes, F. G., *Trans. Am. Soc. Mech. Engrs.*, **73**, 589 (1951).
33. Sherwood, T. K., and R. C. Reid, "The Properties of Gases and Liquids, Their Estimation and Correlation," McGraw-Hill, New York (1958).
34. Vines, R. G., *Australian J. Chem.*, **6**, 1 (1953).
35. Vines, R. G., and L. A. Bennett, *J. Chem. Phys.*, **22**, 360 (1954).
36. Montgomery, J. B., and T. De Vries, *J. Am. Chem. Soc.*, **64**, 2375 (1942).
37. De Vries, T., and B. T. Collins, *ibid.*, **63**, 1343 (1941).
38. Short, W. W., R. A. S. Brown, and B. H. Sage, *J. Applied Mechanics*, **27**, *Trans. Am. Soc. Mech. Engrs.*, Series E, **82**, 393 (1960).
39. Michaud, M., Sc.D. thesis, University of Paris, Paris, France (1951).
40. Sparrow, E. M., and J. L. Gregg, *J. Heat Transfer*, **27**, *Trans. Am. Soc. Mech. Engrs.*, Series C., **82**, (1960).
41. Brown, S. L., *Phys. Rev.*, **21**, (2), 103 (1923).
42. Pei, D. C. T., Calamur Narasimhan, and W. H. Gauvin, Paper presented at the Third Congress of the European Federation of Chemical Engineering London, (June, 1962).
43. Schlichting, Herman, "Boundary Layer Theory," 4th ed., eg. 14.38d, p. 305, McGraw-Hill, New York (1960).

Manuscript received April 11, 1962; revision received November 1, 1962; paper accepted November 1, 1962. Paper presented at A.I.Ch.E. Los Angeles meeting.

The Pumping Capacity of Impellers in Stirred Tanks

GEORGE R. MARR, JR., and ERNEST F. JOHNSON

Princeton University, Princeton, New Jersey

The flow characteristics produced by an impeller in a stirred tank must be known if the overall behavior of the stirred tank is to be predicted. Correlations of impeller power requirements are available for a wide variety of impeller and tank geometries (*1*), but there is relatively little quantitative information about impeller pumping capacities.

Rushton, Mack, and Everett (*4*) attempted the determination of pumping capacities in a special two-tank assembly. Water was pumped by a propeller through an orifice in the bottom of the smaller tank and into the larger surrounding tank. The geometry of the system was adjusted to give a maximum flow, and this maximum flow was assumed to be the actual propeller pumping capacity. These authors found the volumetric pumping rate (q) to be dependent upon the propeller speed (N) and propeller diameter (D_t) according to the equation

$$q = K N D_t^2 \qquad (1)$$

where K is a constant. Some additional data were obtained for turbine impellers with the same experimental technique.

A later paper (*5*) reports the volumetric pumping rate to be dependent on the cube of propeller diameter with the value of K given as 0.4 for water at 70°F.

Sachs and Rushton (*6*) describe a photographic technique that was employed to study both the pumping capacity and the overall circulation caused by turbine impellers. Van de Vusse (*8*) presents a theoretical discussion of the factors defining impeller pumping capacities.

The present paper discusses a new experimental technique for determining pumping capacities. This method is believed to be superior to those previously reported in that it is quite simple and does not disturb the system being studied. Furthermore analysis of the resulting data can give information about overall circulation rates as distinct from pure pumping capacities and point the way to the writing of a mathematical model describing batch mixing experiments and the transient behavior of continuous-flow stirred tanks (*3*).

THE FLOW-TIME DISTRIBUTION EXPERIMENT

The new procedure for studying pumping capacities in stirred tanks involves a flow-time distribution experiment in which the time required for fluid to flow around the circulation pattern of a stirred tank is measured. This measurement is made by watching a small object (called the *flow follower*) as it is carried about the tank and noting each time it passes some chosen reference point. Several hundred observations of this kind are made during one experiment.

Two important conditions must be met if the experimental results are to have a useful meaning. First the flow follower must have the same density as

George R. Marr, Jr., is with the Princeton Computation Center, Princeton, New Jersey.